

Research Article

Surface-Enhanced Raman Scattering of MEH-PPV on Gold and Silver Nanoparticles

Beatriz R. Moraes, Nathalia S. Campos, Alvaro C. C. Barra, and Celly M. S. Izumi 

Laboratório de Nanoestruturas Plasmônicas, Departamento de Química, Universidade Federal de Juiz de Fora, 36036-330 Juiz de Fora, MG, Brazil

Correspondence should be addressed to Celly M. S. Izumi; celly.izumi@ufjf.edu.br

Received 18 December 2017; Accepted 13 February 2018; Published 13 March 2018

Academic Editor: Anatoly Frenkel

Copyright © 2018 Beatriz R. Moraes et al. This is an open access article distributed under the Creative Commons Attribution License, which permits unrestricted use, distribution, and reproduction in any medium, provided the original work is properly cited.

The interaction of poly[2-methoxy-5-(2-ethylhexyloxy)-1,4-phenylenevinylene] (MEH-PPV) with Au or Ag nanospheres, Au nanostars, and Ag nanoprisms was investigated using surface-enhanced Raman scattering (SERS). The SERS investigation showed that adsorption of MEH-PPV strongly depends on the nature of the nanoparticle surface. On gold nanostars that present a thick layer of capping polymer, SERS spectrum is only observed in relatively concentrated MEH-PPV solution (1 mmol L^{-1}). On the other hand, Au and Ag nanospheres present SERS spectra down to $10^{-6} \text{ mol L}^{-1}$ and no chemical interaction of MEH-PPV and metal surface is observed. The spectra of MEH-PPV on Ag nanoprisms with PVP as stabilizing agent suggest that the capping polymer induces a planar conformation of MEH-PPV and consequently an increase of conjugation length. These results give support for the application of MEH-PPV on optoelectronics in which interfacial effects are critical in the device efficiency and stability.

1. Introduction

Poly[2-methoxy-5-(2-ethylhexyloxy)-1,4-phenylenevinylene] (MEH-PPV), structure in Figure 1, is an electroluminescent conjugated polymer that presents improved processability compared to its parent polymer: poly(1,4-phenylenevinylene) (PPV), see also Figure 1 [1, 2]. This class of polymers has attracted interest in fundamental and applied research due to its potential application in photonic and electronic devices such as in light-emitting diodes and photovoltaic cells [3–6].

Although the growing interest in the application of MEH-PPV in optoelectronics, critical challenges concerning the stability and efficiency remain and they are directly related to the interfaces within these devices. In particular, the interface between metal electrodes and the conjugated polymer plays a significant role in the device performance and stability [7, 8]. Additionally, the use of plasmonic nanoparticles (Ag or Au) combined with conjugated polymers has attracted great attention aiming at enhancing their luminescence, resulting in more efficient devices [9–12]. The

performance of solar cells based on conjugated polymers can be also improved by the enhancement of solar harvesting in devices containing Au or Ag nanoparticles [13, 14].

Raman spectroscopy is an important tool for studying the structure of conducting polymers. The correct choice of exciting radiation allows the use of Raman spectroscopy to investigate different chromophoric segments or to probe modifications in the polymer chains after doping [15–17]. Theoretical and experimental vibrational studies of PPV and its oligomers are well reported in the literature describing the structure and the modifications in the neutral and conducting states (*n*-doped and *p*-doped) [18–22]. This vibrational characterization has been extended to the PPV-based polymers such as the MEH-PPV, since the polymer backbones are similar [23–26].

Surface-enhanced Raman scattering (SERS) enables the study of conducting polymers within only a few nanometers around metal nanostructures, and hence, this technique is suitable to probe interfacial effects [27]. The interface between polymer and electrode comprising MEH-PPV and thermal evaporated gold or silver was investigated by SERS,

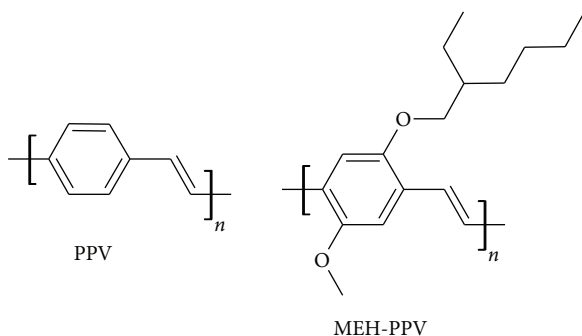


FIGURE 1: Chemical structure of poly[1,4-phenylenevinylene] (PPV) and poly[2-methoxy-5-(2-ethylhexyloxy)-1,4-phenylenevinylene] (MEH-PPV).

showing significant differences between the SERS spectra on these metals assigned to different conformations of MEH-PPV chains [23]. SERS spectra of individual chromophores on single MEH-PPV chains were reported showing two different configurations of the chromophores associated to the packed and loose conformation of the polymer backbone [28].

In this work, we investigated the interaction of MEH-PPV with Ag and Au nanoparticles presenting different morphologies and stabilizing agents using SERS. The SERS spectra of MEH-PPV on these nanoparticles were recorded and the changes in the spectra were correlated with the influence of the nature of the nanoparticle in the structure of the polymer.

2. Materials and Methods

2.1. Materials and Instruments. Poly[2-methoxy-5-(2-ethylhexyloxy)-1,4-phenylenevinylene] (MEH-PPV) (Aldrich) Mn 40–70 kDa, chloroform (Vetec), AgNO_3 (Aldrich), tetrachloroauric acid (Aldrich), polyvinylpyrrolidone (PVP) with average mol wt 40,000 Da (Sigma-Aldrich), *N,N*-dimethylformamide (DMF) (Vetec), and sodium citrate (Sigma-Aldrich) were used as received.

UV–VIS spectra were recorded on a Shimadzu UV-1800 UV–VIS spectrophotometer. Scanning electron microscopy (SEM) was performed on a FEI Magellan scanning electron microscope, with a field emission gun source. Emission spectra were obtained using a Horiba Fluorog3 and a 450 W Xenon lamp as excitation source.

Raman measurements were recorded on a Bruker SENTERRA Raman microscope with a He-Ne laser source at 632.8 nm and a diode laser at 785 nm. The laser beam was focused on the sample by a 50x lens ($\text{NA}=0.51$), and the laser power has always been kept at 0.2 mW in order to avoid sample degradation.

2.2. Synthesis of Silver Nanoparticles

2.2.1. Silver Nanoparticles. Silver nanospheres were prepared following the well-established method described by Creighton et al. using AgNO_3 as silver source and NaBH_4

as reducing agent [29]. UV–VIS spectrum of colloid presents maximum absorption at 398 nm (Supplementary material – Figure S1). This colloid presents silver nanospheres in the range of 1 to 50 nm and borate as primary stabilizing agent [29].

Silver nanoprisms were synthesized in DMF following the procedure described by Pastoriza-Santos and Liz-Marzan [30]. Briefly, 0.160 g of PVP and 0.037 g of AgNO_3 were dissolved in 10 mL of DMF and the mixture was kept under reflux for 30 min. The mixture was centrifuged at 14000 rpm for 10 min, and the solid was dispersed in DMF. UV–VIS spectrum of silver nanoprisms dispersed in DMF is characteristic of triangular nanoprisms with maximum absorptions at 610 nm (Supplementary material – Figure S2). The nanoparticles present mean size of 45 nm and PVP as stabilizing agent.

2.2.2. Gold Nanoparticles. Gold nanospheres were prepared using the method described by Frens [31]. UV–VIS spectrum of gold colloid presents maximum absorption at 522 nm. Typically, this colloid presents spherical nanoparticles with mean diameter of 15 nm (Supplementary material – Figure S3).

Gold nanostars were synthesized following a procedure described by Senthil Kumar et al. [32]. Briefly, Au Frens' colloid was used as seed in DMF solution containing PVP and HAuCl_4 ; after one week, the colloidal suspension becomes blue, indicating the formation of nanostars. UV–VIS spectrum of gold nanostars presents a broad absorption band with maximum at 590 nm (Supplementary material – Figure S4).

2.2.3. SERS Characterization. A stock solution of 1 mg/mL of MEH-PPV in chloroform was prepared; the adequate volume of this solution was mixed with the metal nanoparticles suspensions to obtain the desired polymer concentration. Silver or gold nanoparticle suspensions were incubated for 12 h with MEH-PPV at a final concentration of about 10^{-3} , 10^{-4} , 10^{-5} , and $10^{-6} \text{ mol L}^{-1}$ in which the molarity was calculated on the basis of monomeric units $(\text{C}_{18}\text{H}_{28}\text{O}_2)_n$. After the polymer adsorption, the suspension was centrifuged and rinsed with solvent to remove the remaining solubilized free polymer. The solid was deposited on a glass slide and dried at room temperature.

3. Results and Discussion

3.1. SERS of MEH-PPV on Gold Nanoparticles. Figure 2 presents Raman spectra of MEH-PPV at 633 and 785 nm in the range of 1700 to 900 cm^{-1} , which is dominated by the backbone modes. MEH-PPV presents a strong emission in the range of 500 to 650 nm, overlapping the Raman spectra in visible exciting radiation (Supplementary material – Figure S5). The assignment of vibrational modes was based on previously vibrational studies of PPV and MEH-PPV [18–22, 28]. In the high frequency region, the spectrum at 785 nm presents bands assigned primarily to the backbone modes at 1623 cm^{-1} (vinyl $\nu(\text{C}=\text{C})$), 1581 cm^{-1} (ring $\nu(\text{C}=\text{C})$), 1310 cm^{-1} (vinyl $\nu(\text{C}=\text{C}) + \delta(\text{C}=\text{C}-\text{H})$), 1283 cm^{-1} (ring $\nu(\text{C}=\text{C}) + \delta(\text{C}=\text{C}-\text{H})$), and 967 and 1110 cm^{-1} ($\beta(\text{C}=\text{C}-\text{H})$) [18, 19, 21].

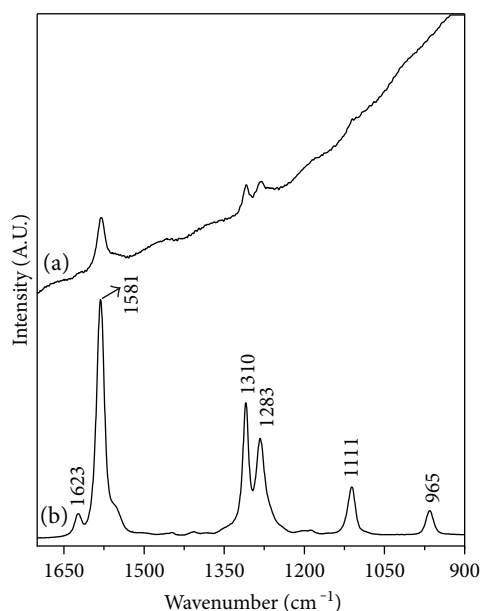


FIGURE 2: Raman spectra of MEH-PPV: (a) $\lambda_0 = 633$ nm and (b) $\lambda_0 = 785$ nm.

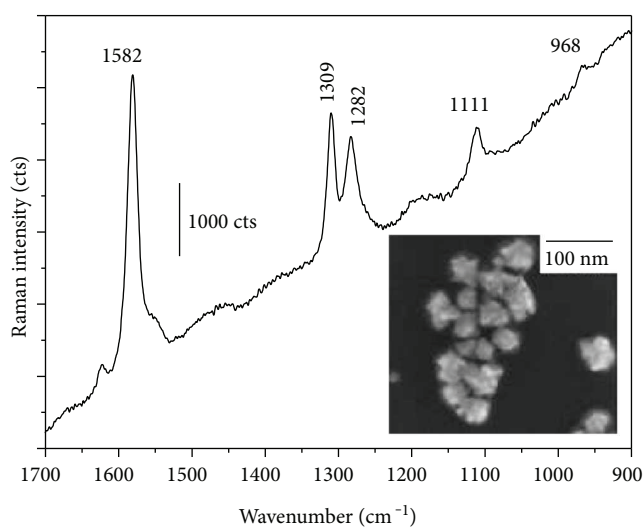


FIGURE 3: SERS spectrum of MEH-PPV on gold nanostars (1×10^{-3} mol L $^{-1}$). $\lambda_0 = 633$ nm. Inset: representative SEM image of gold nanostars.

Figure 3 shows the SERS spectrum of MEH-PPV on gold nanostars. The SERS spectrum resembles the Raman spectrum of the solid MEH-PPV (Figure 2) and is only observed for relatively concentrated MEH-PPV solutions (1×10^{-3} mol L $^{-1}$). These observations can be correlated with SEM images of gold nanostars (inset of Figure 3). Even though these nanoparticles present multiple pods suitable for large SERS enhancement, it is evident that the presence of a PVP layer on gold surface prevents the adsorption of MEH-PPV on the surface, resulting in a SERS spectrum similar to the Raman of the solid polymer. Also, the presence of

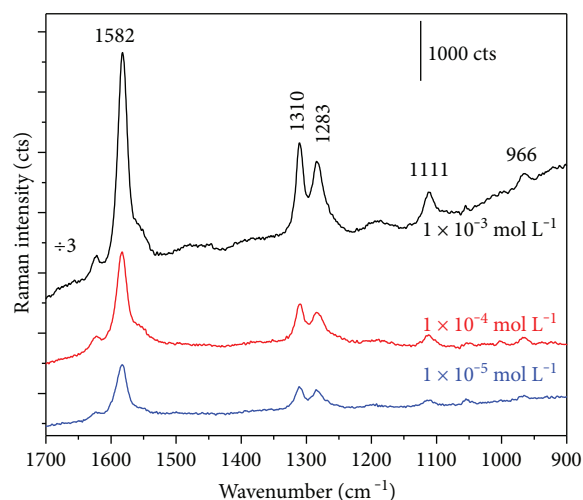


FIGURE 4: SERS spectra of MEH-PPV on gold Frens' colloid at different concentration. $\lambda_0 = 633$ nm.

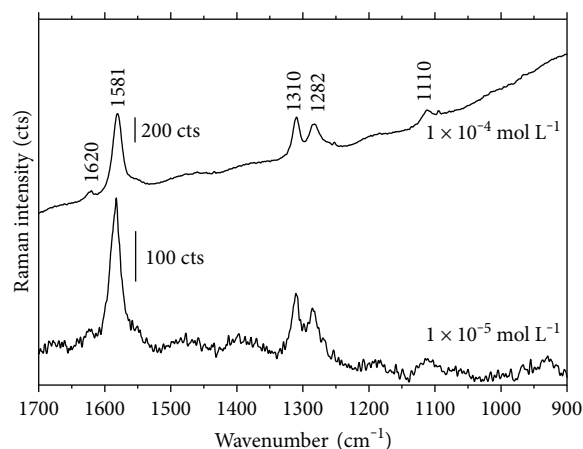


FIGURE 5: SERS spectra of MEH-PPV on silver Creighton's colloid at different concentration. $\lambda_0 = 633$ nm.

the fluorescence background suggests that MEH-PPV is not adsorbed directly on the gold surface; when the polymer is close to the metal surface, its fluorescence is quenched.

Using the 633 nm excitation radiation, SERS spectra of MEH-PPV on gold Frens' colloid are detected for MEH-PPV concentrations down to 1×10^{-5} mol L $^{-1}$ (Figure 4). The fluorescence background is no longer observed due to enhancement of the Raman signal and quenching of fluorescence due to the proximity of MEH-PPV to the gold surface. There is no significant shift of the bands of SERS spectra of MEH-PPV compared to the Raman of solid indicating a lack of chemical interaction to the surface. This result differs to those reported for the SERS of MEH-PPV deposited on gold electrodes in which a new band at 854 cm $^{-1}$ and a decrease in the relative intensity of the bands at about 1300 and 1580 cm $^{-1}$ are observed [23]. The difference between the results indicates that polymer processing, that is, spin coating deposition or adsorption from solution phase and/or the

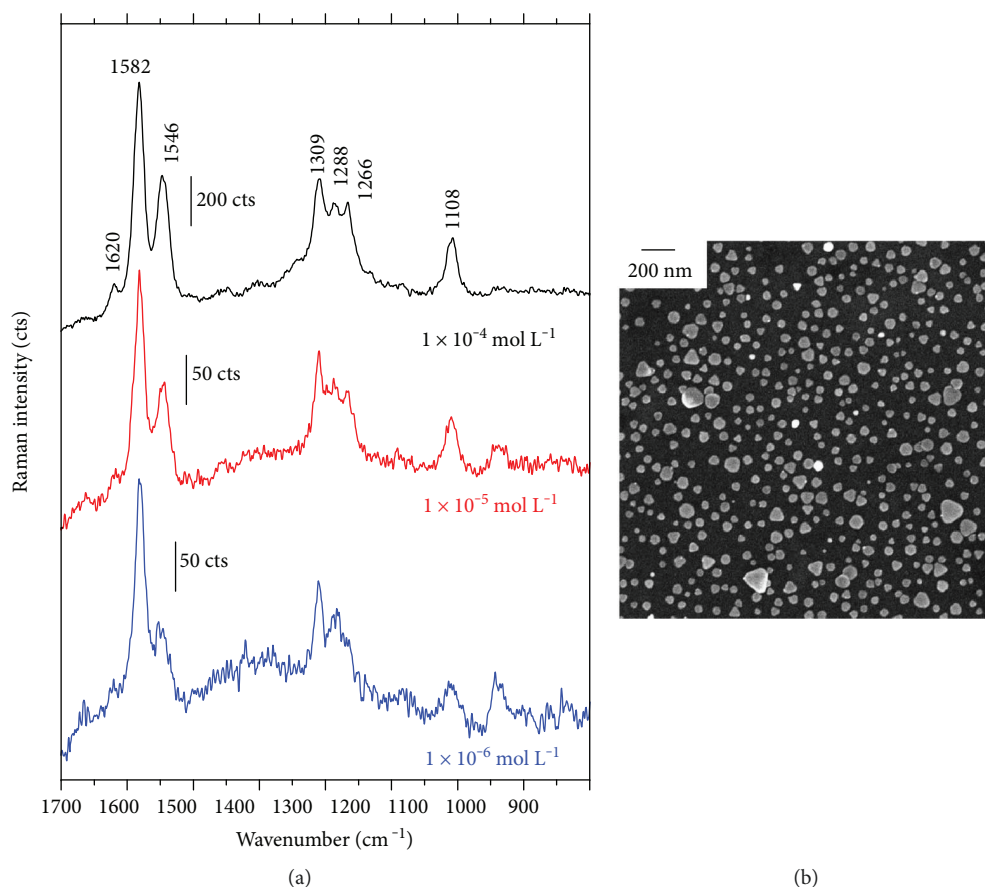


FIGURE 6: (a) SERS spectra of MEH-PPV on silver nanoprisms at different concentration. $\lambda_0 = 633$ nm. (b) Representative SEM image of silver nanoprisms.

nature of gold surface (thermal evaporated gold films or citrate-stabilized gold nanoparticles) play an important role on the structure of MEH-PPV on the metal surface.

3.2. SERS of MEH-PPV on Silver Nanoparticles. The SERS spectra of MEH-PPV on silver Creighton's colloid are shown in Figure 5, and the SERS signal is detected for concentrations down to 10^{-5} mol L $^{-1}$. These spectra are similar to the spectrum of solid MEH-PPV (Figure 2) showing minimal structural variation from the bulk. This is in agreement to the behavior of MEH-PPV deposited on silver electrodes probed by SERS in which no significant spectral variations were observed under excitation at 785 and 532 nm [23]. Fluorescence background is present in the SERS spectrum at 1×10^{-4} mol L $^{-1}$ and it is not observed for the more diluted one. In the samples with higher MEH-PPV concentration, a thicker polymer layer is formed, and the fluorescence quenching is not effective.

The SERS spectra of MEH-PPV on silver nanoprisms are shown in Figure 6(a), the SERS signal is detected for concentrations down to 10^{-6} mol L $^{-1}$. The nanoprisms present mean size of 45 nm (Figure 6(b)) and PVP as stabilizer. In contrast to the SERS of MEH-PPV on silver Creighton's colloid, the spectra of MEH-PPV on silver nanoprisms exhibit notable differences with respect to the solid MEH-PPV.

The difference of SERS spectra of MEH-PPV on Ag nanoprisms and on Creighton's Ag colloid can be attributed to the PVP layer. The PVP-stabilized nanostructures present SERS selectivity due to a discriminatory binding of analytes adsorbed on the polymer layer [33]. There is an enhancement of the band at 1546 cm $^{-1}$, the ratio I_{1546}/I_{1582} is a measure of conjugation length, this ratio increases with the conjugation length. Also, the band observed in the Raman spectrum of the solid (Figure 2) at 966 cm $^{-1}$ is absent in the SERS spectra on silver nanoprisms. This band is assigned to CH out-of-plane wagging and the observation of this band in Raman spectrum is related to the distortion of vinylene groups in PPV chains from a planar form. These results indicate that PVP layer induces the adsorption of MEH-PPV with planar form, consequently with increase of conjugation length. Also, the band at 1266 cm $^{-1}$ in the SERS spectra can be assigned to bipolaronic species, this band is observed in the Raman spectrum of *p*-doped PPV [22]. *P*-type doping of conducting polymers corresponds to an oxidation reaction, this redox reaction can take place on the silver nanoparticle surface; the oxidation of polyaniline on silver nanoparticles was previously detected using SERS [34]. It is important to note that silver surface together with PVP layer induces the adsorption of *p*-doped MEH-PPV chains with higher conjugation length on the metal surface.

4. Conclusion

The SERS spectra of MEH-PPV were recorded in a concentration range of 10^{-3} to 10^{-6} mol L⁻¹ on Au or Ag nanoparticles with different morphology and capping agents. From these SERS results, it appears clear that the adsorption of MEH-PPV strongly depends on the nature of the nanoparticle surface. SERS spectra of MEH-PPV on gold nanostars that present a thick layer of PVP is only observed in relatively concentrated MEH-PPV solution. In contrast, when Au and Ag nanoparticles with citrate or borate as stabilizing agent, respectively, chemical interaction of MEH-PPV and metal surface is not observed in SERS spectra. When Ag nanoparticles with PVP on the surface is used as SERS substrate, MEH-PPV chains present an increase of conjugation length induced by PVP.

Conflicts of Interest

The authors declare that they have no conflicts of interest.

Acknowledgments

The authors gratefully acknowledge the Brazilian agencies Fundação de Amparo à Pesquisa do Estado de Minas Gerais (FAPEMIG), Conselho Nacional de Desenvolvimento Científico e Tecnológico (CNPq), and Coordenação de Aperfeiçoamento de Pessoal de Nível Superior (CAPES) for financial support. The authors thank Dr. Lidia A. Sena and Dr. Bráulio S. Archanjo (Inmetro) for the SEM images of metal nanoparticles. The authors also acknowledge the “Laboratório Interdisciplinar de Eletroquímica e Cerâmica – LIEC” (UFSCar) for the fluorescence spectra of MEH-PPV.

Supplementary Materials

Figure S1: UV-VIS spectrum of silver Creighton's colloid. Figure S2: UV-VIS spectrum of silver nanoprisms. Figure S3: UV-VIS spectrum of gold Frens' colloid. Inset: representative SEM image of gold colloid. Figure S4: UV-VIS spectrum of gold nanostars. Figure S5: Emission spectrum of MEH-PPV in chloroform. $\lambda_{\text{exc}} = 460$ nm. (Supplementary Materials)

References

- [1] J. H. Burroughes, D. D. C. Bradley, A. R. Brown et al., “Light-emitting diodes based on conjugated polymers,” *Nature*, vol. 347, no. 6293, pp. 539–541, 1990.
- [2] D. Braun and A. J. Heeger, “Visible light emission from semiconducting polymer diodes,” *Applied Physics Letters*, vol. 58, no. 18, pp. 1982–1984, 1991.
- [3] L. Akcelrud, “Electroluminescent polymers,” *Progress in Polymer Science*, vol. 28, no. 6, pp. 875–962, 2003.
- [4] Y. Shi, J. Liu, and Y. Yang, “Device performance and polymer morphology in polymer light emitting diodes: the control of thin film morphology and device quantum efficiency,” *Journal of Applied Physics*, vol. 87, no. 9, pp. 4254–4263, 2000.
- [5] G. Yu, J. Gao, J. C. Hummelen, F. Wudl, and A. J. Heeger, “Polymer photovoltaic cells: enhanced efficiencies via a network of internal donor-acceptor heterojunctions,” *Science*, vol. 270, no. 5243, pp. 1789–1791, 1995.
- [6] T. J. Savenije, J. M. Warman, and A. Goossens, “Visible light sensitisation of titanium dioxide using a phenylene vinylene polymer,” *Chemical Physics Letters*, vol. 287, no. 1–2, pp. 148–153, 1998.
- [7] N. Koch, A. Kahn, J. Ghijsen et al., “Conjugated organic molecules on metal versus polymer electrodes: demonstration of a key energy level alignment mechanism,” *Applied Physics Letters*, vol. 82, no. 1, pp. 70–72, 2003.
- [8] Y. Gao, “Surface analytical studies of interfaces in organic semiconductor devices,” *Materials Science and Engineering: R: Reports*, vol. 68, no. 3, pp. 39–87, 2010.
- [9] M. S. Griffo, S. A. Carter, and A. L. Holt, “Enhanced photoluminescence of conjugated polymer thin films on nanostructured silver,” *Journal of Luminescence*, vol. 131, no. 8, pp. 1594–1598, 2011.
- [10] M. S. Kim, D. H. Park, E. H. Cho et al., “Complex nanoparticle of light-emitting MEH-PPV with Au: enhanced luminescence,” *ACS Nano*, vol. 3, no. 6, pp. 1329–1334, 2009.
- [11] G. Saikia, A. Murugadoss, P. J. Sarmah, A. Chattopadhyay, and P. K. Iyer, “Tuning the optical characteristics of poly(*p*-phenylenevinylene) by in situ Au nanoparticle generation,” *The Journal of Physical Chemistry B*, vol. 114, no. 46, pp. 14821–14826, 2010.
- [12] J. Lang, P. Lu, G. Bi, C. Cai, and H. Wu, “Plasmon-enhanced luminescence in novel complex conjugated polymer nanoparticles,” *Optics Letters*, vol. 42, no. 19, pp. 3789–3792, 2017.
- [13] T. Segal-Peretz, O. Sorias, M. Moshonov, I. Deckman, M. Orenstein, and G. L. Frey, “Plasmonic nanoparticle incorporation into inverted hybrid organic–inorganic solar cells,” *Organic Electronics*, vol. 23, pp. 144–150, 2015.
- [14] X. Chen, X. Yang, W. Fu, M. Xu, and H. Chen, “Enhanced performance of polymer solar cells with a monolayer of assembled gold nanoparticle films fabricated by Langmuir–Blodgett technique,” *Materials Science and Engineering: B*, vol. 178, no. 1, pp. 53–59, 2013.
- [15] C. M. S. Izumi, A. M. D. C. Ferreira, V. R. L. Constantino, and M. L. A. Temperini, “Studies on the interaction of emeraldine base polyaniline with Cu(II), Fe(III), and Zn(II) ions in solutions and films,” *Macromolecules*, vol. 40, no. 9, pp. 3204–3212, 2007.
- [16] Y. Furukawa, “Electronic absorption and vibrational spectroscopies of conjugated conducting polymers,” *The Journal of Physical Chemistry*, vol. 100, no. 39, pp. 15644–15653, 1996.
- [17] C. M. S. Izumi, V. R. L. Constantino, and M. L. A. Temperini, “Spectroscopic characterization of polyaniline formed by using copper(II) in homogeneous and MCM-41 molecular sieve media,” *The Journal of Physical Chemistry B*, vol. 109, no. 47, pp. 22131–22140, 2005.
- [18] I. Orion, J. P. Buisson, and S. Lefrant, “Spectroscopic studies of polaronic and bipolaronic species in *n*-doped poly(paraphenylenevinylene),” *Physical Review B*, vol. 57, no. 12, pp. 7050–7065, 1998.
- [19] A. Sakamoto, Y. Furukawa, and M. Tasumi, “Infrared and Raman studies of poly(*p*-phenylenevinylene) and its model compounds,” *The Journal of Physical Chemistry*, vol. 96, no. 3, pp. 1490–1494, 1992.
- [20] S. Lefrant, E. Perrin, J. P. Buisson, H. Eckhardt, and C. C. Han, “Vibrational studies of polyparaphenylene-vinylene (PPV),” *Synthetic Metals*, vol. 29, no. 1, pp. 91–96, 1989.

- [21] E. Mulazzi, A. Ripamonti, J. Wery, B. Dulieu, and S. Lefrant, "Theoretical and experimental investigation of absorption and Raman spectra of poly(paraphenylene vinylene)," *Physical Review B*, vol. 60, no. 24, pp. 16519–16525, 1999.
- [22] M. Baitoul, J. Wéry, J.-P. Buisson et al., "In situ resonant Raman and optical investigations of p-doped poly (*p*-phenylene vinylene)," *Polymer*, vol. 41, no. 18, pp. 6955–6964, 2000.
- [23] D. Li, N. J. Borys, and J. M. Lupton, "Probing the electrode-polymer interface in conjugated polymer devices with surface-enhanced Raman scattering," *Applied Physics Letters*, vol. 100, no. 14, article 141907, 2012.
- [24] M. Baibarac, I. Baltog, I. Smaranda et al., "Spectroelectrochemical properties of the poly[(2,5-bis(octyloxy)-1,4-phenylenevinylene)/single-walled carbon nanotube composite," *Synthetic Metals*, vol. 195, pp. 276–285, 2014.
- [25] A. J. Wise, M. R. Precit, A. M. Papp, and J. K. Grey, "Effect of fullerene intercalation on the conformation and packing of poly-(2-methoxy-5-(3'-7'-dimethyloctyloxy)-1,4-phenylenevinylene)," *ACS Applied Materials & Interfaces*, vol. 3, no. 8, pp. 3011–3019, 2011.
- [26] V. V. Bruevich, T. S. Makhmutov, S. G. Elizarov, E. M. Nechvolodova, and D. Y. Paraschuk, "Raman spectroscopy of intermolecular charge transfer complex between a conjugated polymer and an organic acceptor molecule," *The Journal of Chemical Physics*, vol. 127, no. 10, article 104905, 2007.
- [27] E. C. Le Ru and P. G. Etchegoin, "Chapter 1 – a quick overview of surface-enhanced Raman spectroscopy," in *Principles of Surface-Enhanced Raman Spectroscopy*, pp. 1–27, Elsevier, Amsterdam, Netherlands, 2009.
- [28] Z. Wang and L. J. Rothberg, "Structure and dynamics of single conjugated polymer chromophores by surface-enhanced Raman spectroscopy," *ACS Nano*, vol. 1, no. 4, pp. 299–306, 2007.
- [29] J. A. Creighton, C. G. Blatchford, and M. G. Albrecht, "Plasma resonance enhancement of Raman scattering by pyridine adsorbed on silver or gold sol particles of size comparable to the excitation wavelength," *Journal of the Chemical Society, Faraday Transactions 2: Molecular and Chemical Physics*, vol. 75, p. 790, 1979.
- [30] I. Pastoriza-Santos and L. M. Liz-Marzán, "Synthesis of silver Nanoprisms in DMF," *Nano Letters*, vol. 2, no. 8, pp. 903–905, 2002.
- [31] G. Frens, "Controlled nucleation for the regulation of the particle size in monodisperse gold suspensions," *Nature Physical Science*, vol. 241, no. 105, pp. 20–22, 1973.
- [32] P. Senthil Kumar, I. Pastoriza-Santos, B. Rodríguez-González, F. Javier García de Abajo, and L. M. Liz-Marzán, "High-yield synthesis and optical response of gold nanostars," *Nanotechnology*, vol. 19, no. 1, article 015606, 2008.
- [33] P. Pinkhasova, L. Yang, Y. Zhang, S. Sukhishvili, and H. Du, "Differential SERS activity of gold and silver nanostructures enabled by adsorbed poly(vinylpyrrolidone)," *Langmuir*, vol. 28, no. 5, pp. 2529–2535, 2012.
- [34] C. M. S. Izumi, G. F. S. Andrade, and M. L. A. Temperini, "Surface-enhanced resonance Raman scattering of polyaniline on silver and gold colloids," *The Journal of Physical Chemistry B*, vol. 112, no. 51, pp. 16334–16340, 2008.

